Research Paper

Resting-state connectivity of the bed nucleus of the stria terminalis and the central nucleus of the amygdala in clinical anxiety

Salvatore Torrisi, PhD; Gabriella M. Alvarez, BA; Adam X. Gorka, PhD; Bari Fuchs, BA; Marilla Geraci, MSN; Christian Grillon, PhD*; Monique Ernst, MD, PhD*

Background: The central nucleus of the amygdala and bed nucleus of the stria terminalis are involved primarily in phasic and sustained aversive states. Although both structures have been implicated in pathological anxiety, few studies with a clinical population have specifically focused on them, partly because of their small size. Previous work in our group used high-resolution imaging to map the resting-state functional connectivity of the bed nucleus of the stria terminalis and the central nucleus of the amygdala in healthy subjects at 7 T, confirming and extending structural findings in humans and animals, while providing additional insight into cortical connectivity that is potentially unique to humans. **Methods:** In the current follow-up study, we contrasted resting-state functional connectivity in the bed nucleus of the stria terminalis and central nucleus of the amygdala at 7 T between healthy volunteers (n = 30) and patients with generalized and/or social anxiety disorder (n = 30). **Results:** Results revealed significant voxel-level group differences. Compared with healthy volunteers, patients showed stronger resting-state functional connectivity between the central nucleus of the amygdala and the lateral orbitofrontal cortex and superior temporal sulcus. They also showed weaker resting-state functional connectivity between the bed nucleus of the stria terminalis and the dorsolateral prefrontal cortex and occipital cortex. **Limitations:** These findings depart from a previous report of resting-state functional connectivity in the central nucleus of the amygdala and bed nucleus of the stria terminalis under sustained threat of shock in healthy volunteers. **Conclusion:** This study provides functional MRI proxies of the functional dissociation of the bed nucleus of the stria terminalis and central nucleus of the amygdala, and suggests that resting-state functional connectivity of key structures in the processing of defensive responses do not recapitulate changes related to induced state anxiety. Future work needs to replicate and further probe the clinical significance of these findings.

Introduction

Anxiety disorders exact a heavy individual and societal burden.[1,2] Although psychological and pharmacological treatments are available, they are not always effective.[3] A better understanding of the neural mechanisms that underlie these disorders should help to develop more optimal, targeted therapeutic approaches.

The present work focuses on 2 key subcortical brain structures of the extended amygdala:[4] the bed nucleus of the stria terminalis (BNST) and the central nucleus of the amygdala (CeA). These regions are histologically related,[5] and they are structurally and metabolically connected.[6–8] They have been proposed to serve distinct functions in the processing of defensive responses, which are of 2 broad types: fear (transient automatic response to proximal threat) and anxiety (sustained, deliberate response to distal threat). Generally, the BNST has been associated with anxiety, and the CeA has been associated with fear.[9–11] It is reasonable to expect that this functional specialization would be reflected at the level of neural networks, which can be probed using resting-state functional MRI (fMRI).[12]

Information about anxiety-related networks can be garnered from a substantial literature of neurobehavioural studies in animals[13,14] and neuroimaging studies in humans.[15–17] However, the relevance to humans of insight derived from animal models is inherently limited by the absence of measures that capture symptoms of psychopathology (e.g., worry), as well as by the difficulty of assessing small subcortical structures in humans using standard MRI

Correspondence to: S. Torrisi, Building 15K, Room 203, National Institute of Mental Health, Bethesda, MD, 20814; sam.torrisi@nih.gov

*These authors contributed equally to this work.

Submitted Sep. 2, 2018; Revised Dec. 11, 2018; Accepted Jan. 16, 2019; Published online Apr. 9, 2019

DOI: 10.1503/jpn.180150

scanners. Indeed, most human studies have examined the whole amygdala, ignoring its partitions into functionally distinct subnuclei. This approach may have contributed to inconsistent findings across research groups. Studies tend to concur that the recruitment of regions modulated by (or that modulate) the coding of threat in the amygdala are perturbed in patients with anxiety disorders.[18–20] For example, Prater and colleagues[20] observed weaker connectivity between the amygdala and the rostral anterior cingulate cortex (ACC) at rest, as well as in a psychophysiological interaction analysis with fearful face matching, in patients with social anxiety disorder (SAD) compared with healthy people. Similarly, Etkin and colleagues[21] observed hypoconnectivity between the amygdala and the ACC at rest in patients with generalized anxiety disorder. Other studies, however, have reported stronger functional connectivity between the amygdala and this area in anxious patients (SAD).[22] These results indicate that the nature of amygdala connectivity in anxiety disorders remains inconsistent and in need of further investigation. Furthermore, the significance of stronger versus weaker resting-state functional connectivity is still under debate. Generically, stronger resting-state functional connectivity reflects tighter coupling, and weaker resting-state functional connectivity reflects poorer, more inefficient, coupling. However, a number of considerations challenge these one-to-one associations,[23] and interpretations should exhibit prudence.

There is a lack of studies examining resting-state BNST connectivity in anxiety disorders. Andreescu and colleagues[24] found that self-reported measures of "somatic anxiety" were associated with increased connectivity between the BNST and left temporal gyrus, while "global anxiety" was associated with increased connectivity between the BNST and left frontal and temporal cortices.

Most models place the initial processing of threat in the amygdala and consider the regions that modulate and are modulated by this structure. Broadly, these regions are found in the medial prefrontal cortex (mPFC), which is involved in emotion valuation and regulation;[25] the parietal cortex, which is involved in the modulation of attention;[26] and the dorsolateral prefrontal cortex (dlPFC), which is involved in executive control.[27]

Using threat of shock as an experimental tool in healthy participants,[28] our group has focused on the cortical regions that are engaged in induced state anxiety, including the dlPFC, the dorsomedial prefrontal cortex (dmPFC) and the dorsal frontoparietal attention network. We found that the dlPFC reflected the engagement of executive-control processes to reduce state anxiety,[29,30] the dmPFC to update and regulate emotional valuation,[31,32] and the dorsal frontoparietal attention network to gate attention to relevant stimuli.[33] Interestingly, clinical anxiety showed weak recruitment of the dlPFC, a region identified during an induced anxious state,[29] but has shown strong engagement of the dorsal ACC/dmPFC, an area identified in the expression of anxiety.[34,35] These findings delineate key neural regions that contribute to the processing of anxiety, but they leave gaps, such as the contribution of small structures known from animal work to be of central importance in the coding of anxiety: that is, the BNST and CeA.

The goal of the present work is to begin to fill these important gaps. In a series of resting-state studies using ultra-high-field fMRI, our laboratory described the functional connectivity profiles of the BNST and CeA, particularly as they relate to the functional neural networks affected by clinical anxiety disorders. Two studies in healthy participants revealed both common and distinct functional connectivity patterns between these 2 regions.[36,37] Both regions evidenced strong coupling with the ventromedial prefrontal cortex (vmPFC), an area consistently reported in fear conditioning and fear extinction.[38] Overall, the BNST showed robust coupling with regions that support cognitive and motivational processing, and the CeA was tightly coupled with regions that support sensory processing.[36] The most recent study examined the effect of experimentally induced anxiety evoked by threat of shock.[39] Threat manipulation mostly reduced the coupling of the BNST and CeA with regions involved in emotional valuation and motivation (i.e., the vmPFC, ACC and nucleus accumbens). However, increased positive connectivity during threat was also observed between the CeA and anterior thalamus. The current study explored resting-state connectivity among patients with generalized anxiety disorder (GAD) and/or SAD compared with healthy volunteers. We selected these 2 disorders because they are highly prevalent and comorbid.[40]

This brief background suggests 2 main hypotheses. First, distinct patterns of abnormal resting-state functional connectivity of the BNST and the CeA are expected to emerge in people with clinical anxiety. These abnormalities would refine previously reported connectivity findings of the whole amygdala. More specifically, we would expect the functional connectivity patterns of the CeA (concerned with transient, automatic threat response) and the BNST (concerned with sustained, reflective threat response) to be observable. Accordingly, the more direct, automatic mechanisms of emotion valuation and inhibition (supported by regions of the inferior/ventral prefrontal cortex [PFC]) would interact preferentially with the CeA, and the more cognitive, sustained mechanisms of strategic emotion regulation (supported by regions such as the ventrolateral PFC and hippocampus) would interact preferentially with the BNST. Second, based on a relative predominance of fMRI findings that report lower amygdala connectivity with the PFC in anxiety,[18,41,42] we would predict lower connectivity in anxious patients than in healthy volunteers. However, given the inconsistent findings in the literature, we might uncover more complex patterns of greater and lesser couplings in anxious patients.[43,44] We might also expect findings in clinical anxiety to replicate our previous findings of CeA and BNST resting-state functional connectivity under threat of shock in healthy people. If this hypothesis is correct, abnormal networks could support both a propensity for experiencing anxiety (clinical trait anxiety) and expressing anxiety (state anxiety). If incorrect, trait anxiety could be linked to abnormal networks responsible for the propensity for but not the expression of the anxiety state.

Methods

Participants

We recruited patients through public advertisements in newspapers, campus flyers and online sites (Craigslist). An experienced psychiatric nurse evaluated all participants who reported anxiety symptoms using the Structured Clinical Interview for DSM-IV-TR, Patient Edition (SCID).[45] Patients who met the criteria for an anxiety disorder were evaluated by a senior psychiatrist to confirm the DSM-IV diagnosis. Participants were enrolled in the study if they were diagnosed with GAD and/or SAD (among the most common anxiety diagnoses), if they were matching healthy participants and if they met inclusion criteria. Participants were excluded if they met the following criteria: current Axis I disorders other than anxiety; use of psychopharmacological medications that alter central nervous system function within 2 weeks of the experiment; braces, permanent retainer or metal implants; head trauma with loss of consciousness greater than 5 minutes; or substance abuse or dependence within 6 months. Excessive head motion during the functional imaging runs was also an exclusion criterion. This was defined as greater than 15% of a participant's repetition times censored ("scrubbed"), where the criterion for censoring was motion derivative greater than 0.3 mm for temporally adjacent time points. Remaining head motion across scans (number of censored time points) was also tested between groups with a Welch 2-sample, 2-tailed t test and was not significantly different between groups: healthy participants (mean ± standard deviation) = 2.66 ± 5.1; patients = 1.8 ± 3.0; $p = 0.39$. The analyses contrasted the healthy participant and patient groups in total, because the high number of comorbid GAD/SAD participants precluded analyses of patient subgroups. Participants provided written informed consent in accordance with the institutional review board at the National Institute of Mental Health.

Data acquisition

We collected data using a 7 T Siemens Magnetom MRI and a 32-channel head coil. The high-resolution, 0.7 mm isotropic, T_1-weighted structural scan had the following parameters: repetition time 2200 ms, echo time 3.01, flip angle 7°, acquisition time 10 min. The functional echo-planar imaging had the following parameters: interleaved repetition time 2.5 s, echo time 27 ms, flip angle 70°, 49 slices, 1.3 mm isotropic voxels, 240 images collected over a 10-minute scan. The echo-planar imaging field of view collected was approximately two-thirds of the brain, angled to capture the dmPFC, BNST, amygdala and hippocampus while minimizing signal dropout and eye-movement artifacts. We collected physiologic (cardiac and respiratory) recordings using a BioPac MP150 system set at 500 Hz (www.biopac.com). Participants were given earplugs and head pads to further control movement and sound, and a pillow was placed under their legs for comfort and stability. Participants were instructed to keep their eyes open and look at a white fixation cross on a black background.

Immediately after the scan and while still in the scanner, participants completed the validated Amsterdam Resting-State Questionnaire (ARSQ) version 2.0[46] in E-Prime (Psychology Software Tools, Inc.) to assess levels of sleepiness. We included this questionnaire as a quality-control check, because sleepiness can affect brain network function.[47]

Mask definitions

Bilateral BNST masks were defined individually for each participant using a previously described protocol.[37] Briefly, 3 raters (S.T., G.A., B.F.) manually drew BNSTs in Analysis of Functional Neuroimages (AFNI)[48] on high-resolution structural scans using anatomic landmarks as boundaries (e.g., lateral ventricle, anterior commissure, thalamostriate vein). After a preliminary trial period with test data, the drawing order of subjects for each rater was randomized to spread further learning effects across the samples. Each individual BNST (left and right separately defined) was then averaged among the 3 raters and thresholded at two-thirds in a kind of voting procedure. This resulted in binary masks for everyone, from which we pulled averaged time series. Because some of the acquired data had been published previously, 2 of 3 raters were different for the patient set (G.A., B.F.) than for the healthy volunteer set (K.O., A.D.; see Acknowledgements), although some healthy volunteers were included in the drawing pool to blind raters to diagnosis. We also acquired data from 11 new healthy volunteers, interleaved with patient acquisition, to better match age and sex demographics. In other words, 2 earlier studies from our group consisted of a healthy volunteer cohort ($n = 27$),[36,37] and 19 of those participants were used in the present study. Eleven new participants were added to the 19 healthy volunteers to optimize matching of the healthy volunteer and patient groups in terms of demographic variables ($n = 30$ for each group). Only after these demographic measures were matched between groups, incorporating head-motion quality control, did we perform analyses. However, because of personnel turnover, 6 of the newly acquired healthy volunteers' BNSTs were drawn by a single rater (ST).

The bilateral CeA mask was chosen from probabilistic masks of amygdala subregions in Montreal Neurological Institute (MNI) space created from a large, high-resolution, multimodal 7 T data set.[49] We visually checked alignment of this mask against our group-level, nonlinearly normalized anatomy and deemed it to be very accurate.

Thresholded and volumetrically rendered versions of both the BNST and CeA masks are shown in their anatomic context in Figure 1. We also extracted participant-specific parcellations of the primary auditory cortex (A1; e.g., Mišic and colleagues[50]) as a "control region" whose functional connectivity was not expected to differ between groups.

Preprocessing and analyses

Preprocessing began with FreeSurfer tissue segmentation and parcellations;[51] subsequent preprocessing and analyses continued in AFNI. The initial 3 repetition times of the functional

run were discarded to allow for steady-state equilibrium. Functional volumes for each participant were slice-time-corrected, motion-corrected, realigned and coregistered to their corresponding T_1-weighted structural image. Structural scans were nonlinearly normalized using 3dQwarp to the MNI/ICBM 2009b Nonlinear, Asymmetric template.[52] The resulting parameters were then applied to the cortical parcellations and functional volumes, the latter being spatially smoothed with a kernel of 2.6 mm (full width at half maximum), as previously done.[36,37] We made a mask for group analyses by intersecting 2 images: a binarized mask of 95% echo-planar imaging of all participants and a probabilistic grey-matter map derived from the normalization template, which itself was binarized at 25% (Appendix 1, Fig. S1, available at jpn.ca/180150-a1).

Resting-state data can be deleteriously affected by physiologic noise, which must be removed before analysis. The following nuisance signals were regressed from the functional data: (1) 6 head-motion parameters and first derivatives, (2) 5 slice-based respiration regressors,[53] (3) 8 slice-based cardiac regressors,[54] (4) time series extracted from eroded masks of the lateral third and fourth ventricle, (5) time series from white matter within local spheres (13 mm radius) surrounding each voxel using ANATICOR,[55] and (6) 0.01–0.1 Hz bandpass filter regressors. We extracted average time series in the BNST, CeA and A1 masks from the image residuals. Pearson correlations between each ROI time series and all other voxels in the brain mask were calculated and Fisher-transformed for group analyses.

These images were then entered into 2-sample, 2-tailed t tests to determine voxels that exhibited intrinsic resting-state functional connectivity that was significantly different between groups. All group-level statistical maps were thresholded at $p < 0.05$ and whole-brain corrected using a cluster-defining threshold of $p < 0.005$, $\kappa = 70$, using 3dClustSim's acf autocorrelation function.[56] To help interpret notions of "hypo-" or "hyper-" connectivity in the final group comparisons, we also extracted mean correlations from significant clusters using 3dROIstats and we graphed them in R version 3.4.2.[57]

We also calculated explanatory post hoc correlations between self-reports and voxel-level brain connectivity, separate from the 2-sample t tests described above. Missing self-report data (< 5% for the Beck Anxiety Inventory [BAI][58] and Liebowitz Social Anxiety Scale [LSAS][59]) was handled through multiple imputation by chained equations (MICE),[60] version 2.46, in R,[57] with custom scripts that pooled 3dttest++ estimates and variances into t statistics with per-voxel-adjusted degrees of freedom.[61] The t statistic maps were then transformed to z statistics and corrected for multiple comparisons at the whole-brain level. Finally, these corrected clusters were binarized into masks for correlation extraction at the single-participant level to be entered into group (patients) correlation analyses with the self-report measures.

Results

Demographics, sleepiness

The healthy volunteer group ($n = 30$) and the patient group ($n = 30$) were demographically matched in terms of age, sex, socioeconomic status and IQ (Wechsler Abbreviated Scale of Intelligence[62]). An independent χ^2 test for race categories (white, black, Asian, Hispanic/other) was not significant: $\chi^2_3 = 4.9$, $p = 0.18$ (Table 1). As assessed using the Amsterdam Resting-State Questionnaire, sleepiness during the resting scan was not significantly different between groups ($p = 0.53$).

Functional neuroimaging

Overall, across the acquired field of view, statistically significant group differences in resting-state functional connectivity were limited to 6 clusters for the BNST and 2 clusters for the CeA.

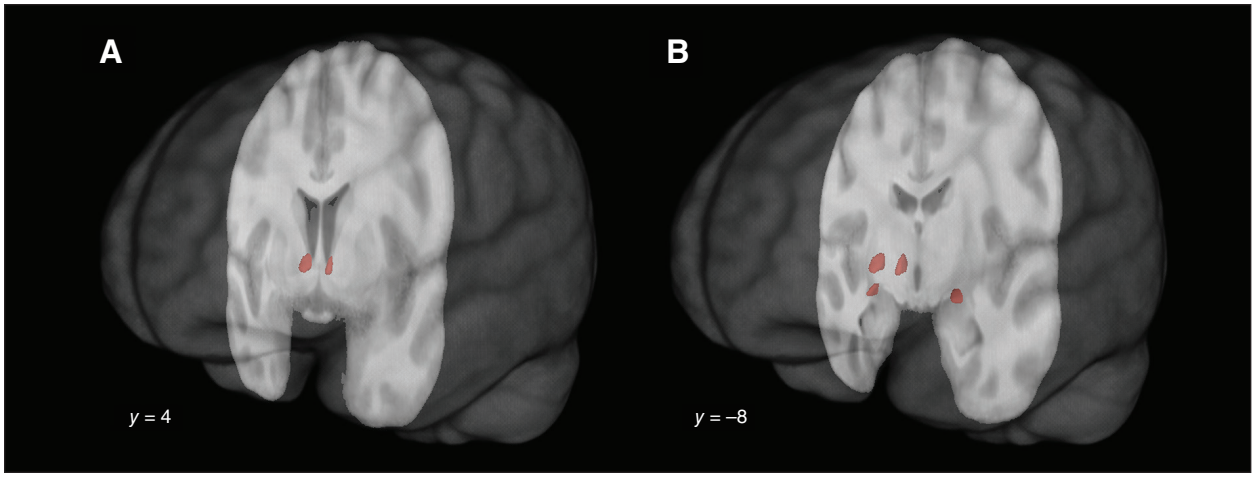

Fig. 1: Extended amygdala masks in oblique, left-hemisphere views through a translucent, group-averaged brain. (A) Coronal slice through probabilistic BNST mask thresholded at 50%. (B) A more posterior coronal slice through (maximum probability map) CeA. Visualized with SUMA in AFNI. BNST = bed nucleus of the stria terminalis; CeA = central nucleus of the amygdala.

The 6 clusters exhibiting group differences for the BNST were found in the dlPFC (left and right dlPFC: Brodmann area [BA] 6 and BA9; left middle frontal gyrus, left inferior frontal gyrus: BA44) and the lateral occipital cortex (left and right, BA18; Fig. 2 and Table 2). These group differences indicated hypoconnectivity in patients relative to healthy volunteers (Fig. 3A).

The 2 clusters revealing group differences for the CeA were found in the right lateral orbitofrontal cortex (lOFC, BA47) and the right anterior superior temporal sulcus (aSTS, BA22; Fig. 4 and Table 2). These group differences indicated hyperconnectivity in patients, but no correlation between CeA and these regions in healthy volunteers (Fig. 3B).

Table 1: Participant characteristics*

Characteristic	Healthy volunteers (*n* = 30)	Patients (*n* = 30)	*p* value
Age, yr	29.51 ± 7.2	29.46 ± 7.8	NS
Female, *n* (%)	22 (73)	22 (73)	NS
Race, *n*			
White	14	19	NS
Black	4	6	NS
Asian	8	2	NS
Hispanic/other	4	3	NS
HH SES	46.33	45.04	NS
WASI	117.63	117.86	NS
GAD diagnosis, *n* (%)	—	8 (27)	—
SAD diagnosis, *n* (%)	—	8 (27)	—
Mixed diagnosis, *n* (%)†	—	14 (47)	—
LSAS (total)	14.67 ± 13.3	70.79 ± 24	< 0.001
STAI‡	24.57 ± 4.6	41.73 ± 8.2	< 0.001
BAI	1.23 ± 2.2	10.17 ± 7.6	< 0.001

BAI = Beck Anxiety Inventory; GAD = generalized anxiety disorder; HH SES = Hollingshead Social Economic Status; LSAS = Liebowitz Social Anxiety Scale; NS = not significant; SAD = social anxiety disorder; STAI = State-Trait Anxiety Inventory; WASI = Wechsler Abbreviated Scale of Intelligence.
*Values are mean ± standard deviation unless otherwise indicated; *t* tests were 2-sample, 2-tailed, unequal variance.
†GAD + SAD or GAD + SAD + panic disorder (*n* = 2 for latter).
‡Administered before scanning.

As expected, we found no significant differences between groups in the connectivity of the control (auditory) region A1. Within-group maps replicated previous work[36,37] (Appendix 1).

Post hoc brain–behaviour analyses

We assessed correlations with anxiety ratings on 2 commonly used and well-validated scales. Scores on the BAI[58] and the LSAS[59] were correlated with resting-state functional connectivity of the BNST and CeA. These analyses were conducted only in the anxiety group because of the low variability of these ratings in the healthy volunteer group.

With respect to resting-state functional connectivity in the BNST, the BAI was positively correlated with a cluster in the precuneus (Fig. 5A/B; $r = 0.497$; $p = 0.005$), such that higher anxiety ratings were associated with stronger BNST–precuneus coupling. With respect to resting-state functional connectivity in the CeA, the LSAS was positively correlated with a cluster in the mPFC (Fig. 5C/D; $r = 0.585$; $p < 0.001$), such that higher anxiety ratings were associated with stronger CeA–mPFC coupling.

Discussion

This study examined how resting-state functional connectivity of the 2 principal nodes of the extended amygdala network — the BNST and the CeA — differed in patients with anxiety disorders compared to healthy volunteers. To our knowledge, this is the first study to address this question using ultra-high-field data, which allows us to reliably examine small structures and their connectivity. Findings revealed both predicted and novel information about the patterns of resting-state networks of the extended amygdala regions in patients with anxiety disorders. Three points will be discussed. First, we address the resting-state functional connectivity regions that are sensitive to group differences. Second, we consider the directions of these group differences. Third, we comment on the results of the exploratory analyses of brain–behaviour associations.

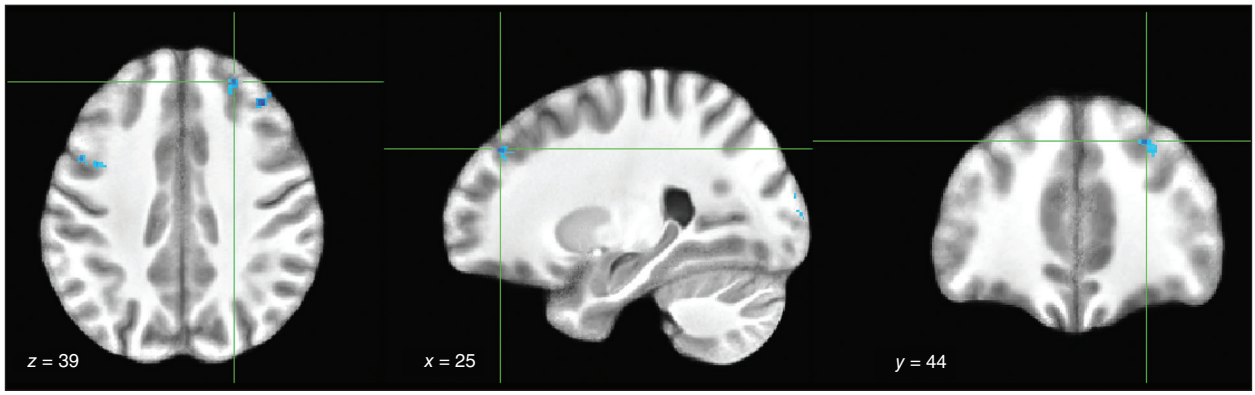

Fig. 2: Connectivity, BNST; patients greater than healthy volunteers. Axial, sagittal and coronal slices. Negative *t* statistics are blue. Crosshairs at 1 of 3 main prefrontal results (dorsolateral prefrontal cortex). Cluster-defining threshold $p = 0.005$, $\kappa = 70$, corrected at $p < 0.05$. Also visualized on the group average of all participants' nonlinearly normalized structural scans. BNST = bed nucleus of the stria terminalis.

First, as expected, resting-state functional connectivity for both the BNST and the CeA showed distinct perturbations in patients with anxiety disorders compared with healthy volunteers. Overall, findings were consistent with the proposed functional specialization of these nodes.

The CeA acts as the output nucleus of the amygdala, channelling emotional and social information to be processed into phasic behavioural responses (e.g., fear responses). The anxiety group showed alterations of CeA resting-state functional connectivity with the lateral OFC (which supports emotional valuation and regulation[25]) and the superior temporal sulcus (which mediates social perception and cognition via multisensory integration[63]). These findings might underlie the exaggerated automatic responses to emotional/social information

Table 2: Coordinates of peak voxels, patients versus controls

Region	MNI coordinates, *x, y, z*	Cluster size in voxels	Peak *t* statistic
BNST connectivity			
Right lateral occipital (BA18)	30.2, –92.1, 14.8	171	–5.1
Right middle frontal gyrus (BA9)	35.2, 31.6, 32.2	156	–5.33
Left middle frontal gyrus (BA6)	–48.5, 6.6, 38.5	105	–3.94
Left lateral occipital (BA18)	–26, –95.9, 16	85	–4.24
Left inferior frontal gyrus (BA44)	–41, 5.4, 24.8	84	–4.1
Right superior frontal gyrus (BA9)	25.2, 44.1, 38.5	74	–4.12
CeA connectivity			
Right lateral orbitofrontal (BA47)	36.5, 32.9, –17.8	80	4.52
Superior temporal sulcus (BA22)	60.2, –3.4, –15.2	87	4.42

BA = Brodmann area; BNST = bed nucleus of the stria terminalis; CeA = central nucleus of the amygdala; MNI = Montreal Neurological Institute.
$p < 0.005$, $\kappa = 70$; 2-sided, NN = 2, acf corrected.

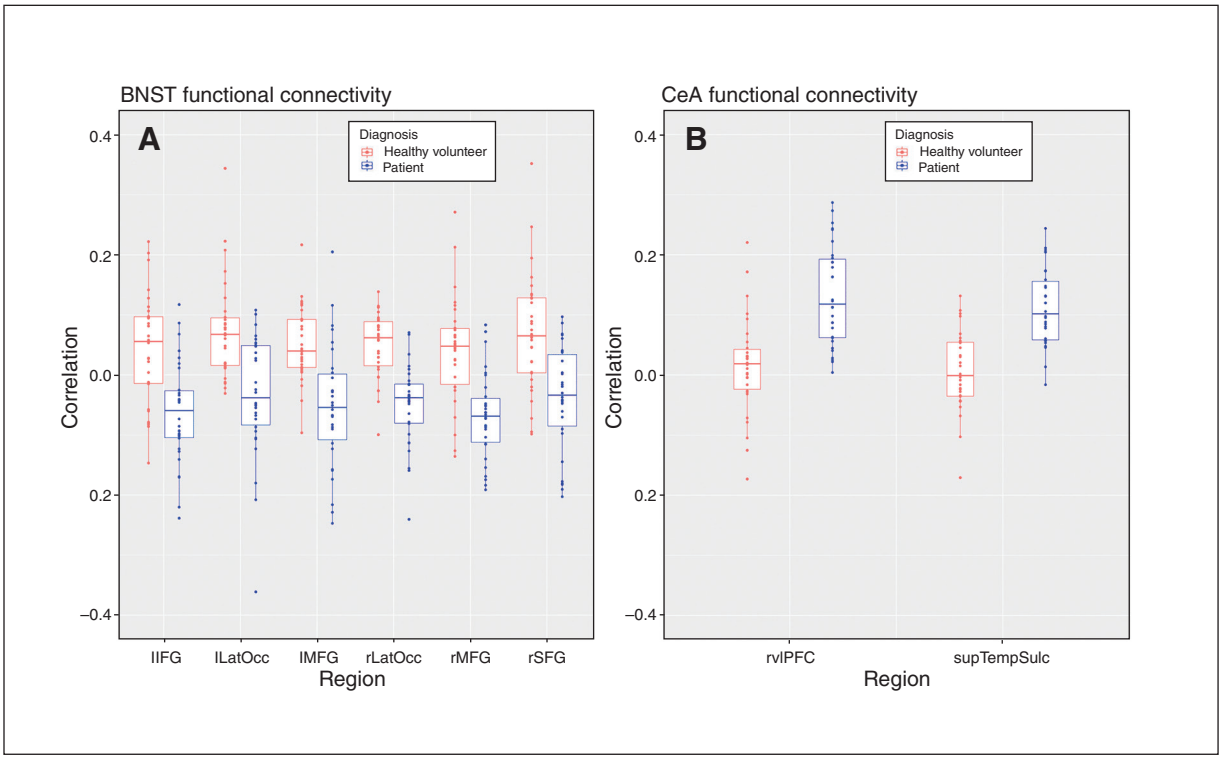

Fig. 3: Parsing the voxel-level maps, patients > healthy volunteers. Correlations extracted from significant clusters are reported in Table 2, with regional abbreviations referencing the same regions. (A) Correlations with BNST. (B) Correlations with CeA. Visualized on the group average of all participants' nonlinearly normalized structural scans. BNST = bed nucleus of the stria terminalis; CeA = central nucleus of the amygdala; lIFG = left inferior frontal gyrus; lLatOcc = left lateral occipital cortex; lMFG = left medial frontal gyrus; rLatOcc = right lateral occipital cortex; rMFG = right medial frontal gyrus; rSFG = right superior frontal gyrus; supTempSulc = superior temporal sulcus; rvlPFC = right ventrolateral prefrontal cortex.

displayed in anxiety disorders. Of note, these findings differed from previous work that assessed these connectivities in healthy participants during sustained threat of shock and safety.[39,64] Consequently, clinical anxiety does not recapitulate state anxiety at the level of resting-state functional connectivity in the CeA.

The BNST, working in tandem with the amygdala, integrates sensory, social and emotional information into deliberate motivated behaviours (e.g., anxiety responses). As such, we expected perturbations of resting-state functional connectivity in the BNST to affect regions involved in high-order cognitive function. In line with this notion, patients with anxiety exhibited abnormal BNST coupling with the dlPFC, a structure associated with working memory and emotion-regulation strategies such as reappraisal.[65] In previous work, threat of shock in healthy volunteers was similarly associated with reduced resting-state functional connectivity in the BNST. However, the specific paths involved in state anxiety (threat of shock) differed from those found here in anxious patients.

Interestingly, resting-state fMRI studies have shown significant coupling between the BNST and the hippocampus,[37,66] and among the BNST, CeA and hippocampus.[36,67] Our findings did not detect any effects of pathological anxiety on hippocampal-extended amygdala couplings. This null result echoes the absence of effects of induced anxiety (via threat of shock) on these circuits in healthy participants.[39] Conceivably, the hippocampus engagement in anxiety disorders requires an active challenge, such as fear learning or threat detection. Accordingly, human studies have shown transient (rather than sustained) hippocampal activation during anxiogenic context conditioning,[68,69] which may not be observable under resting conditions. More work is needed to tease apart these possibilities.

Taken together, the present findings indicate that the resting-state functional connectivity circuits of the CeA and BNST are sensitive to clinical anxiety but differ from those affected by state anxiety in healthy people. This discrepancy opens interesting prospects to better understand the vulnerability mechanisms that underlie excessive state anxiety. One possibility is that the current findings might offer insights into how the CeA and BNST prime the neural paths that directly respond to anxiogenic situations, and that these neural paths are dysfunctional in people with anxiety. Such speculation could be tested in future work by comparing people with anxiety and healthy volunteers during the states of threat of shock and safety. However, it is also possible that the neural network responsible for pathological anxiety in GAD and SAD differs from the one that mediates response to sustained threat of shock. Indeed, psychophysiology studies show no exaggerated defensive responses to sustained threat of shock in people with GAD and SAD.[70,71] Future studies should examine whether resting-state functional connectivity of the CeA and BNST in anxious patients who do show excessive defensive response to sustained threat of shock (i.e., patients with posttraumatic stress disorder or panic disorder[70,72]) is similar to the resting-state functional connectivity of threat of shock.

Not expected in patients with anxiety was the abnormal coupling of the BNST with the visual association areas (BA18) of the occipital cortex. This deviation might be related to an anxiety-related biased interpretation of visual stimuli as excessively negative, or salient, which characterizes anxious cognition.[73] Although this interpretation is speculative, it is interesting in relation to literature that describes the amygdala's involvement in perception.[74,75]

The second point of this discussion concerns the direction of these disrupted couplings in anxiety patients compared with healthy volunteers. Findings revealed that all the BNST group differences reflected weaker functional connectivity in the patient group than in the healthy volunteer group. However, the opposite was true for the CeA clusters of resting-state functional connectivity, for which group differences reflected stronger connectivity in the patient group. The task-based and resting-state fMRI literature

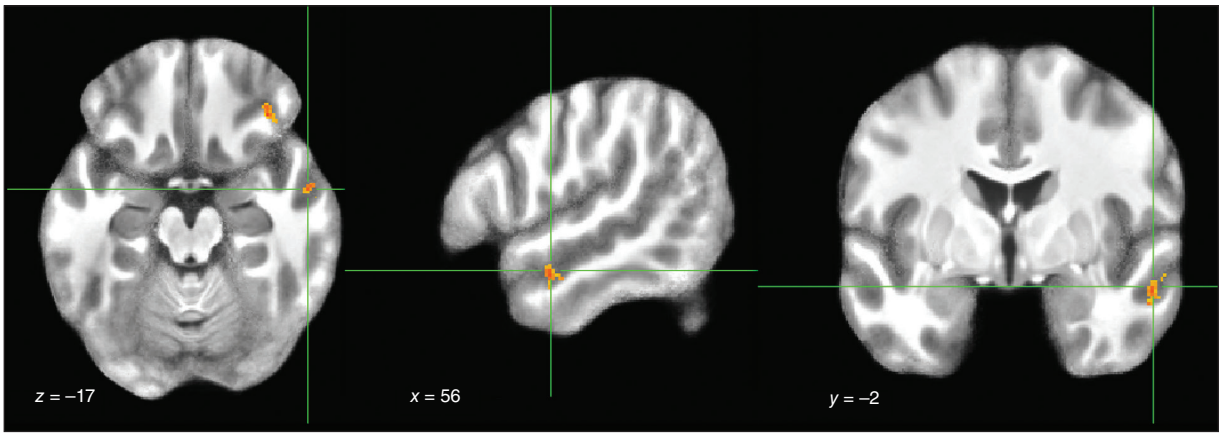

Fig. 4: Connectivity, CeA; patients > healthy volunteers. Axial, sagittal and coronal slices. Crosshairs at superior temporal sulcus. Also shown in axial slice is lateral orbitofrontal cortex. Cluster-defining threshold $p = 0.005$, $\kappa = 70$, corrected at $p < 0.05$. Visualized on the group average of all participants' nonlinearly normalized structural scans. CeA = central nucleus of the amygdala.

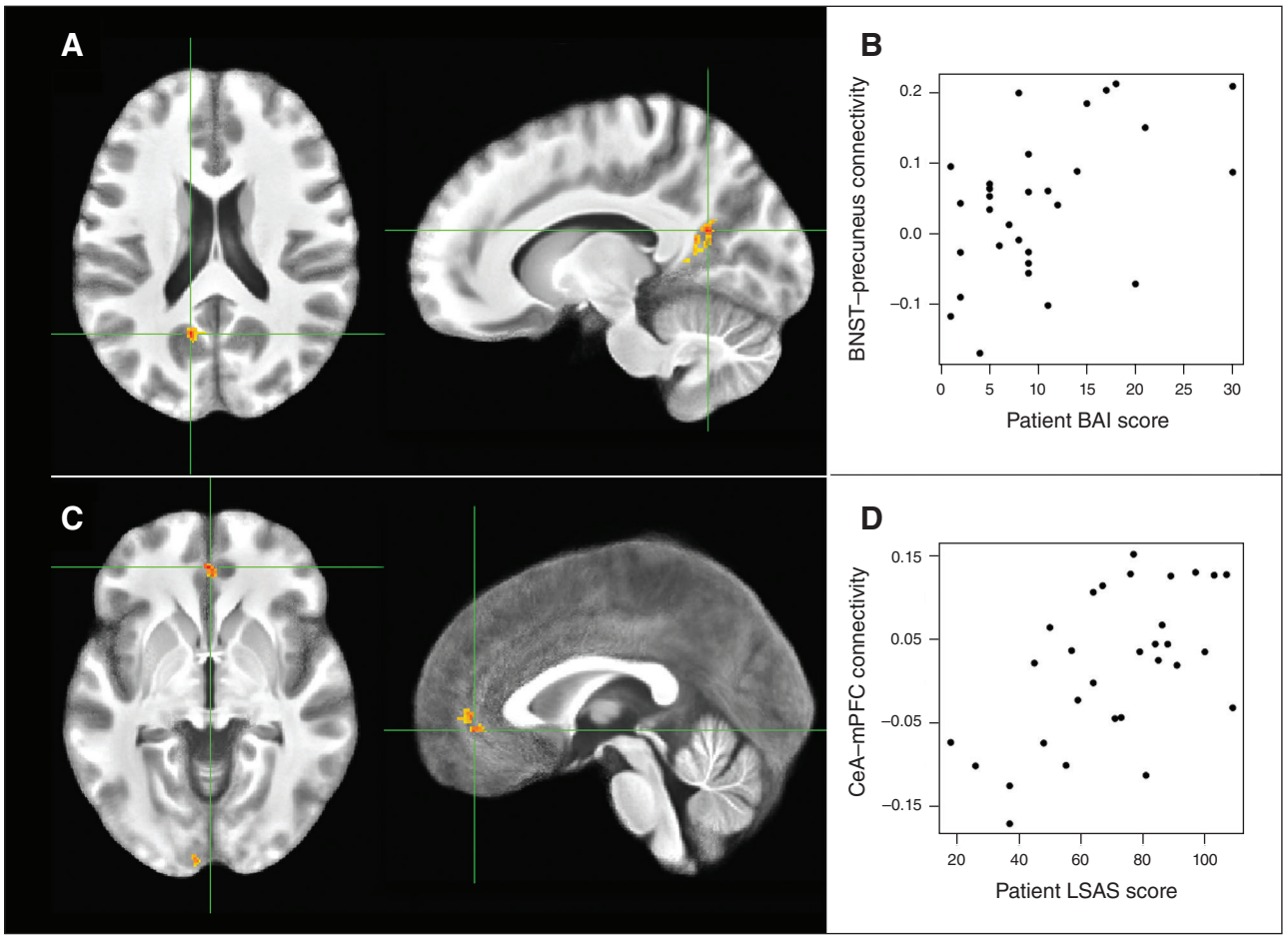

Fig. 5: Connectivity correlations with patient self-report. (A, B) Correlations between BNST and precuneus/posterior cingulate connectivity and BAI scores in patients. (C, D) Correlations between CeA and medial PFC connectivity and LSAS scores in patients. BAI = Beck Anxiety Inventory; BNST = bed nucleus of the stria terminalis; CeA = central nucleus of the amygdala; LSAS = Liebowitz Social Anxiety Scale; PFC = prefrontal cortex.

more frequently reports lower (whole) amygdala connectivity with PFC regions in people with anxiety compared to healthy people.[17,21,76,77] However, anxiety-related higher amygdala connectivity has also been described, particularly with the ventral and medial PFC regions.[78–80] The opposite effects of diagnosis status on the direction of CeA (higher) and BNST (lower) resting-state functional connectivity can be interpreted in various ways. First, the present correlation analysis to measure connectivity is the standard, static Pearson correlation. This type of analysis does not detect underlying dynamic fluctuations.[81] Therefore, it is conceivable that critical but transient fluctuations in BNST couplings may occur in patients, lowering correlations across the entire time series. Another possibility for hypoconnectivity with patients' BNST may be related to the recruitment of additional brain regions under threat, which could divert processing resources away from "optimally" shortest paths.[82] In other words, the BNST findings in patients may reflect more diffuse and variable patterns of communication with regions that underlie higher cognitive function and visual attention. Yet another possibility may be a regional change at the neural level in response timing, information processing, transmission efficacy or even neurovascular coupling, which could manifest as a shift in phase between blood-oxygenation-level-dependent signals and a decrease in correlations.[83] These interpretations should be tested in future work that can probe these functions using task-based fMRI and other types of analyses.

Finally, the third category of findings stems from our exploratory examination of brain–behaviour correlations in the anxiety group. We used 2 anxiety self-reports: the BAI, which probes somatic symptoms of anxiety, and the LSAS, which is specific to social anxiety. The BNST–precuneus resting-state functional connectivity was positively correlated with the BAI ($p < 0.005$). This finding suggests that patients with clinical anxiety maintain tight communication between the BNST and a region involved in attention, self-referential thinking and visuospatial processing. None of the BNST resting-state functional connectivity clusters (dlPFC, lOCC) that distinguished patients from healthy volunteers in the main analyses were correlated with BAI or LSAS scores. Of note, these clusters were weakly coupled in patients (i.e., significantly

weaker than in healthy volunteers), and thus poorly engaged during the resting-state scan, which may explain the absence of correlations with a self-report measure. The CeA–mPFC resting-state functional connectivity was positively correlated with LSAS scores ($p < 0.001$), but not with BAI scores. This mPFC cluster was found in the pregenual area, which is thought to regulate brain areas that generate behavioural responses to emotions (e.g., amygdala, hypothalamus, periaqueductal grey).[84] This region is also involved in computing values of decisions, including social decisions.[85,86] Therefore, the stronger association of CeA–mPFC coupling with more severe social anxiety symptoms on the LSAS might reflect the greater taxing of this functional path in people with anxiety, supporting the maintenance of active automatic modulation of responses to emotions, as well as the excessive salience of social motivated behaviour. The absence of significant correlations between the CeA clusters sensitive to group differences (lOFC, aSTS) and symptom severity might reflect a mode of functioning in anxious patients rather than more direct substrates of symptoms. This interpretation is consistent with the different findings of state anxiety by threat of shock in healthy people and the present findings of trait anxiety.

Limitations

A few limitations to the present study should be mentioned. First, sex effects could not be reliably assessed because of the unbalanced proportion of females to males in the sample. Exploratory analyses on sex differences were not conclusive and were underpowered. Second, the assessment of specific contributions of distinct anxiety disorders (e.g., GAD v. SAD) was not possible because of their high comorbidity across our patients. The examination of diagnostic types should be a next step, particularly since the brain–behaviour exploratory analysis identified distinct pathways correlated with social anxiety symptom severity (LSAS) and somatic anxiety (BAI). Third, to achieve the highest spatial resolution with the techniques available at the time of data acquisition, the field of view did not include the whole brain, excluding most of the dorsal cortex and ventral cerebellum (Appendix 1). This means that the dorsal connectivity shown in other, whole-brain BNST and CeA resting-state studies with healthy participants could not be tested in the present patient population.[66,67] This limitation will be mitigated with newer data acquisition strategies, such as simultaneous multi-slice acquisition.[87] Fourth, the BNST masks could not resolve BNST subdivisions;[88] however, they included mostly the lateral subregion, which is the BNST component most implicated in anxiogenic processes.[9] Finally, although the plots in Fig. 3 help clarify the nature of the group differences, any such interpretive phrasing such as "hypo-" or "hyper-" connectivity is at this point speculative, given the nature of resting blood-oxygenation level–dependent findings.[23] Insight into a clearer etiology for group differences shown here could be tested in future studies using task-based designs, effective connectivity analyses and/or other imaging modalities.

Conclusion

Findings support the functional dissociation of the 2 nodes of the extended amygdala, the BNST and CeA, which engaged distinct abnormal paths in clinical anxiety. The paths engaged by the BNST might be related more closely to networks involved in cognitive regulation of anxiety (weaker coupling in patients than in healthy volunteers), whereas those engaged by the CeA might preferentially involve automatic value coding and regulation (stronger coupling in patients than in healthy volunteers). These findings are important for guiding future work to extend and better understand the role of the extended amygdala in pathological anxiety.

Acknowledgements: This research was supported (in part) by the Intramural Research Program of the National Institute of Mental Health. The authors thank Katherine O'Connell and Andrew Davis for assistance with data collection, Nicholas Balderston for manuscript commentary, and Gang Chen and Justin Rajendra for guidance with statistical imputation. This work used the computational resources of the National Institutes of Health HPC Biowulf cluster (http://hpc.nih.gov). This work was supported by the Intramural Research Program of the National Institute of Mental Health, project number ZIAMH002798 (clinical protocol 02-M-0321, NCT00047853) to C. Grillon.

Affiliations: From the Section on the Neurobiology of Fear and Anxiety, National Institute of Mental Health, Bethesda, MD, USA (Torrisi, Alvarez, Gorka, Fuchs, Geraci, Grillon, Ernst).

Competing interests: None declared.

Contributors: S. Torrisi, C. Grillon and M. Ernst designed the study. S. Torrisi, G. Alvarez, B. Fuchs and M. Geraci acquired the data, which S. Torrisi, G. Alvarez, A. Gorka, B. Fuchs, C. Grillon and M. Ernst analyzed. S. Torrisi, G. Alvarez, C. Grillon and M. Ernst wrote the article, which all authors reviewed. All authors approved the final version to be published and can certify that no other individuals not listed as authors have made substantial contributions to the paper.

References

1. Craske MG, Stein MB, Eley TC, et al. Anxiety disorders. *Nat Rev Dis Primers* 2017;3:1-18.
2. Wittchen HU, Jacobi F, Rehm J, et al. The size and burden of mental disorders and other disorders of the brain in Europe 2010. *Eur Neuropsychopharmacol* 2011;21:655-79.
3. Koen N, Stein DJ. Pharmacotherapy of anxiety disorders: a critical review. *Dialogues Clin Neurosci* 2011;13:423-37.
4. Heimer L, Van Hoesen GW, Trimble M, et al. *Anatomy of neuropsychiatry: the new anatomy of the basal forebrain and its implications for neuropsychiatric illness*. 1st ed. Cambridge (MA): Academic Press; 2007.
5. Walter A, Mai JK, Lanta L, et al. Differential distribution of immunohistochemical markers in the bed nucleus of the stria terminalis in the human brain. *J Chem Neuroanat* 1991;4:281-98.
6. DeCampo DM, Fudge JL. Amygdala projections to the lateral bed nucleus of the stria terminalis in the macaque: comparison with ventral striatal afferents. *J Comp Neurol* 2013;521:3191-216.
7. Kruger O, Shiozawa T, Kreifelts B, et al. Three distinct fiber pathways of the bed nucleus of the stria terminalis to the amygdala and prefrontal cortex. *Cortex* 2015;66:60-8.
8. Oler JA, Birn RM, Patriat R, et al. Evidence for coordinated functional activity within the extended amygdala of non-human and human primates. *Neuroimage* 2012;61:1059-66.

9. Davis M, Walker DL, Miles L, et al. Phasic vs sustained fear in rats and humans: role of the extended amygdala in fear vs anxiety. *Neuropsychopharmacology* 2010;35:105-35.
10. Avery SN, Clauss JA, Blackford JU. The human BNST: functional role in anxiety and addiction. *Neuropsychopharmacology* 2016;41:126-41.
11. Shackman AJ, Fox AS. Contributions of the central extended amygdala to fear and anxiety. *J Neurosci* 2016;36:8050-63.
12. Zhang D, Raichle ME. Disease and the brain's dark energy. *Nat Rev Neurol* 2010;6:15-28.
13. Lang PJ, Davis M, Ohman A. Fear and anxiety: animal models and human cognitive psychophysiology. *J Affect Disord* 2000;61:137-59.
14. Kumar V, Bhat ZA, Kumar D. Animal models of anxiety: a comprehensive review. *J Pharmacol Toxicol Methods* 2013;68:175-83.
15. Blackford JU, Pine DS. Neural substrates of childhood anxiety disorders: a review of neuroimaging findings. *Child Adolesc Psychiatr Clin N Am* 2012;21:501-25.
16. Sylvester CM, Corbetta M, Raichle ME, et al. Functional network dysfunction in anxiety and anxiety disorders. *Trends Neurosci* 2012;35:527-35.
17. Hilbert K, Lueken U, Beesdo-Baum K. Neural structures, functioning and connectivity in generalized anxiety disorder and interaction with neuroendocrine systems: a systematic review. *J Affect Disord* 2014;158:114-26.
18. Kim MJ, Loucks RA, Palmer AL, et al. The structural and functional connectivity of the amygdala: from normal emotion to pathological anxiety. *Behav Brain Res* 2011;223:403-10.
19. Maslowsky J, Mogg K, Bradley BP, et al. A preliminary investigation of neural correlates of treatment in adolescents with generalized anxiety disorder. *J Child Adolesc Psychopharmacol* 2010;20:105-11.
20. Prater KE, Hosanagar A, Klumpp H, et al. Aberrant amygdala-frontal cortex connectivity during perception of fearful faces and at rest in generalized social anxiety disorder. *Depress Anxiety* 2013;30:234-41.
21. Etkin A, Prater KE, Schatzberg AF, et al. Disrupted amygdalar subregion functional connectivity and evidence of a compensatory network in generalized anxiety disorder. *Arch Gen Psychiatry* 2009;66:1361-72.
22. Anteraper SA, Triantafyllou C, Sawyer AT, et al. Hyper-connectivity of subcortical resting-state networks in social anxiety disorder. *Brain Connect* 2014;4:81-90.
23. Hall CN, Howarth C, Kurth-Nelson Z, et al. Interpreting BOLD: towards a dialogue between cognitive and cellular neuroscience. *Philos Trans R Soc Lond B Biol Sci* 2016;371:pii 20150348.
24. Andreescu C, Mennin D, Tudorascu D, et al. The many faces of anxiety-neurobiological correlates of anxiety phenotypes. *Psychiatry Res* 2015;234:96-105.
25. Ochsner KN, Gross JJ. The cognitive control of emotion. *Trends Cogn Sci* 2005;9:242-9.
26. Han S. The role of human parietal cortex in attention networks. *Brain* 2003;127:650-9.
27. Ballard IC, Murty VP, Carter RM, et al. Dorsolateral prefrontal cortex drives mesolimbic dopaminergic regions to initiate motivated behavior. *J Neurosci* 2011;31:10340-6.
28. Schmitz A, Grillon C. Assessing fear and anxiety in humans using the threat of predictable and unpredictable aversive events (the NPU-threat test). *Nat Protoc* 2012;7:527-32.
29. Balderston N, Vytal KE, O'Connell K, et al. Anxiety patients show reduced working memory related DLPFC activation during safety and threat. *Depress Anxiety* 2016;34:25-36.
30. Balderston N, Quispe-Escudero D, Hale E, et al. Working memory maintenance is sufficient to reduce state anxiety. *Psychophysiology* 2016;53:1660-68.
31. Robinson OJ, Charney DR, Overstreet C, et al. The adaptive threat bias in anxiety: amygdala–dorsomedial prefrontal cortex coupling and aversive amplification. *Neuroimage* 2012;60:523-9.
32. Robinson OJ, Krimsky M, Lieberman L, et al. The dorsal medial prefrontal (anterior cingulate) cortex–amygdala aversive amplification circuit in unmedicated generalised and social anxiety disorders: an observational study. *Lancet Psychiatry* 2014;1:294-302.
33. Balderston N, Hale E, Hsiung A, et al. Threat of shock increases excitability and connectivity of the intraparietal sulcus. *Elife* 2017;6:e23608.
34. Shin LM, Davis FC, VanElzakker MB, et al. Neuroimaging predictors of treatment response in anxiety disorders. *Biol Mood Anxiety Disord* 2013;3:1-11.
35. Milad MR, Pitman RK, Ellis CB, et al. Neurobiological basis of failure to recall extinction memory in posttraumatic stress disorder. *Biol Psychiatry* 2009;66:1075-82.
36. Gorka AX, Torrisi SJ, Shackman AJ, et al. Intrinsic functional connectivity of the central nucleus of the amygdala and bed nucleus of the stria terminalis. *Neuroimage* 2018;168:392-402.
37. Torrisi SJ, O'Connell K, Davis A, et al. Resting state connectivity of the bed nucleus of the stria terminalis at ultra-high field. *Hum Brain Mapp* 2015;36:4076-88.
38. Giustino TF, Maren S. The role of the medial prefrontal cortex in the conditioning and extinction of fear. *Front Behav Neurosci* 2015;9:758-20.
39. Torrisi SJ, Gorka AX, Gonzalez-Castillo J, et al. Extended amygdala connectivity changes during sustained shock anticipation. *Transl Psychiatry* 2018;8:1-12.
40. Kessler RC, Chiu WT, Demler O, et al. Prevalence, severity, and comorbidity of 12-month DSM-IV disorders in the national comorbidity survey replication. *Arch Gen Psychiatry* 2005;62:617-20.
41. He Y, Xu T, Zhang W, et al. Lifespan anxiety is reflected in human amygdala cortical connectivity. *Hum Brain Mapp* 2015;37:1178-93.
42. Etkin A, Prater KE, Hoeft F, et al. Failure of anterior cingulate activation and connectivity with the amygdala during implicit regulation of emotional processing in generalized anxiety disorder. *Am J Psychiatry* 2010;167:545-54.
43. Hamm LL, Jacobs RH, Johnson MW, et al. Aberrant amygdala functional connectivity at rest in pediatric anxiety disorders. *Biol Mood Anxiety Disord* 2014;4:1-9.
44. Williams LM. Defining biotypes for depression and anxiety based on large-scale circuit dysfunction: a theoretical review of the evidence and future directions for clinical translation. *Depress Anxiety* 2017;34:9-24.
45. First MB, Spitzer RL, Gibbon M, et al. *Structured clinical interview for DSM-IV-TR Axis I disorders—non-patient edition.* New York: Biometrics Research, New York State Psychiatric Institute; 2007.
46. Diaz BA, Van Der Sluis S, Benjamins JS, et al. The ARSQ 2.0 reveals age and personality effects on mind-wandering experiences. *Front Psychol* 2014;5:271.
47. Tagliazucchi E, Laufs H. Decoding wakefulness levels from typical fMRI resting-state data reveals reliable drifts between wakefulness and sleep. *Neuron* 2014;82:695-708.
48. Cox RW. AFNI: software for analysis and visualization of functional magnetic resonance neuroimages. *Comput Biomed Res* 1996;29:162-73.
49. Tyszka JM, Pauli WM. In vivo delineation of subdivisions of the human amygdaloid complex in a high-resolution group template. *Hum Brain Mapp* 2016;37:3979-98.
50. Mišic B, Betzel RF, Griffa A, et al. Network-based asymmetry of the human auditory system. *Cereb Cortex* 2018;28:2655-64.
51. Fischl B. FreeSurfer. *Neuroimage* 2012;62:774-81.
52. Fonov V, Evans AC, Botteron K, et al. Unbiased average age-appropriate atlases for pediatric studies. *Neuroimage* 2011;54:313-27.
53. Birn RM, Smith MA, Jones TB, et al. The respiration response function: the temporal dynamics of fMRI signal fluctuations related to changes in respiration. *Neuroimage* 2008;40:644-54.

54. Glover GH, Li TQ, Ress D. Image-based method for retrospective correction of physiological motion effects in fMRI: RETROICOR. *Magn Reson Med* 2000;44:162-7.

55. Jo HJ, Saad ZS, Simmons WK, et al. Mapping sources of correlation in resting state fMRI, with artifact detection and removal. *Neuroimage* 2010;52:571-82.

56. Cox RW, Chen G, Glen DR, et al. fMRI clustering and false-positive rates. *Proc Natl Acad Sci U S A* 2017;114:E3370-1.

57. *R: A language and environment for statistical computing*. Vienna, Austria: R Core Team; 2016. Available: www.R-project.org (accessed 2019 Mar. 22).

58. Beck AT, Epstein N, Brown G, et al. An inventory for measuring clinical anxiety: psychometric properties. *J Consult Clin Psychol* 1988;56:893-7.

59. Liebowitz M. Social phobia. *Mod Probl Pharmacopsychiatry* 1987;22: 141-73.

60. van Buuren S, Groothuis-Oudshoorn K. Mice: multivariate imputation by chained equations in R. *J Stat Softw* 2011;45:1-67.

61. Barnard J, Rubin DB. Small-sample degrees of freedom with multiple imputation. *Biometrika* 1999;86:948-55.

62. Wechsler D. *Manual for the Wechsler Adult Intelligence Scale*. Oxford: Psychological Corp; 1955.

63. Deen B, Koldewyn K, Kanwisher N, et al. Functional organization of social perception and cognition in the superior temporal sulcus. *Cereb Cortex* 2015;25:4596-609.

64. Vytal KE, Overstreet C, Charney D, et al. Sustained anxiety increases amygdala–dorsomedial prefrontal coupling: a mechanism for maintaining an anxious state in healthy adults. *J Psychiatry Neurosci* 2014;39:321-9.

65. Ochsner KN, Silvers JA, Buhle JT. Functional imaging studies of emotion regulation: a synthetic review and evolving model of the cognitive control of emotion. *Ann N Y Acad Sci* 2012;1251:E1-24.

66. Avery SN, Clauss JA, Winder DG, et al. BNST neurocircuitry in humans. *Neuroimage* 2014;91:311-23.

67. Tillman RM, Stockbridge MD, Nacewicz BM, et al. Intrinsic functional connectivity of the central extended amygdala. *Hum Brain Mapp* 2017;39:1654-22.

68. Alvarez RP, Biggs A, Chen G, et al. Contextual fear conditioning in humans: cortical-hippocampal and amygdala contributions. *J Neurosci* 2008;28:6211-9.

69. Marschner A, Kalisch R, Vervliet B, et al. Dissociable roles for the hippocampus and the amygdala in human cued versus context fear conditioning. *J Neurosci* 2008;28:9030-6.

70. Grillon C, Pine DS, Lissek S, et al. Increased anxiety during anticipation of unpredictable aversive stimuli in posttraumatic stress disorder but not in generalized anxiety disorder. *Biol Psychiatry* 2009;66:47-53.

71. Grillon C, O'Connell K, Lieberman L, et al. Distinct responses to predictable and unpredictable threat in anxiety pathologies: effect of panic attack. *Biol Psychiatry Cogn Neurosci Neuroimaging* 2017;2:575-81.

72. Grillon C, Lissek S, Rabin S, et al. Increased anxiety during anticipation of unpredictable but not predictable aversive stimuli as a psychophysiologic marker of panic disorder. *Am J Psychiatry* 2008; 165:898-904.

73. Robinson OJ, Vytal KE, Cornwell BR, et al. The impact of anxiety upon cognition: perspectives from human threat of shock studies. *Front Hum Neurosci* 2013;7:1-21.

74. Vuilleumier P, Armony JL, Driver J, et al. Effects of attention and emotion on face processing in the human brain an event-related fMRI study. *Neuron* 2001;30:829-41.

75. Pessoa L, McKenna M, Gutierrez E, et al. Neural processing of emotional faces requires attention. *Proc Natl Acad Sci U S A* 2002; 99:11458-63.

76. McClure EB, Monk CS, Nelson EE, et al. Abnormal attention modulation of fear circuit function in pediatric generalized anxiety disorder. *Arch Gen Psychiatry* 2007;64:97-106.

77. Qiao J, Li A, Cao C, et al. Aberrant functional network connectivity as a biomarker of generalized anxiety disorder. *Front Hum Neurosci* 2017;11:626.

78. Guyer AE, Lau JYF, McClure-Tone EB, et al. Amygdala and ventrolateral prefrontal cortex function during anticipated peer evaluation in pediatric social anxiety. *Arch Gen Psychiatry* 2008;65:1303-12.

79. Jalbrzikowski M, Larsen B, Hallquist MN, et al. Development of white matter microstructure and intrinsic functional connectivity between the amygdala and ventromedial prefrontal cortex: associations with anxiety and depression. *Biol Psychiatry* 2017;82:511-21.

80. Roy AK, Fudge JL, Kelly C, et al. Intrinsic functional connectivity of amygdala-based networks in adolescent generalized anxiety disorder. *J Am Acad Child Adolesc Psychiatry* 2013;52:290-2.

81. Hutchison RM, Womelsdorf T, Allen EA, et al. Dynamic functional connectivity: promise, issues, and interpretations. *Neuroimage* 2013;80:360-78.

82. Avena-Koenigsberger A, Mišic B, Hawkins RXD, et al. Path ensembles and a tradeoff between communication efficiency and resilience in the human connectome. *Brain Struct Funct* 2017;222:603-18.

83. Stephan KE. On the role of general system theory for functional neuroimaging. *J Anat* 2004;205:443-70.

84. Etkin A, Egner T, Kalisch R. Emotional processing in anterior cingulate and medial prefrontal cortex. *Trends Cogn Sci* 2011;15:85-93.

85. Rilling JK, Sanfey AG. The neuroscience of social decision-making. *Annu Rev Psychol* 2011;62:23-48.

86. Lee VK, Harris LT. How social cognition can inform social decision making. *Front Neurosci* 2013;7:259.

87. Setsompop K, Gagoski BA, Polimeni JR, et al. Blipped-controlled aliasing in parallel imaging for simultaneous multislice echo planar imaging with reduced g-factor penalty. *Magn Reson Med* 2012; 67:1210-24.

88. Dong H-WW, Petrovich GD, Swanson LW. Topography of projections from amygdala to bed nuclei of the stria terminalis. *Brain Res Brain Res Rev* 2001;38:192-246.